Soil Dynamics and Earthquake Engineering 144 (2021) 106654

Contents lists available at ScienceDirect

Soil Dynamics and Earthquake Engineering

journal homepage: http://www.elsevier.com/locate/soildyn

Seismic performance of steel moment frames considering the effects of column-base hysteretic behavior and gravity framing system

Pablo Torres-Rodas [a,*], Francisco Flores [b,c], Sebastian Pozo [b], Bryam X. Astudillo [b]

[a] College of Science and Engineering, Universidad San Francisco de Quito, Ecuador
[b] Department of Civil Engineering, Universidad de Cuenca, Ecuador
[c] Department of Civil Engineering, Universidad Del Azuay, Ecuador

A B S T R A C T

This paper presents a parametric study conducted on five Steel Moment Frames (SMFs) varying in height (2-, 4-, 8-, 12-, and 20- story) to assess the interactive effect of the column base hysteretic behavior, continuous gravity columns and partially restrained gravity beam-column connections in their seismic performance. The frame response is examined through sophisticated Nonlinear Time History (NTH) and Nonlinear Static Pushover (NSP) analyses conducted as per FEMAp695 methodology. For each SMF, a range of base connection strengths (and their corresponding rotational stiffnesses) accompanied by different levels of gravity columns rigidity and gravity connection strengths are assigned, resulting in a total of 80 model simulations. Two collapse/failure limit states are formulated for the assessment 1) sidesway collapse defined as per FEMAp695; and 2) column-base connection failure, defined as base rotations exceeding a 0.05 rad threshold. Results from the simulations indicate that the gravity framing system profoundly affects the behavior of the SMFs analyzed by reducing their probability of collapse. In this manner, the seismic demands for the design of column-base connections can be reduced safely, incorporating their high deformation capacity as part of the energy dissipative mechanisms. Potential design implications are discussed, and limitations, as well as lines for future research, are outlined.

1. Introduction

Steel Moment Frames (SMFs) are one of the most common lateral-load resisting systems in seismically active regions such as the West Coast of the United States or Japan. Because of it, their seismic performance has been extensively studied over the last decades. Experimental evidence demonstrates that SMFs are among the most ductile lateral-load resisting systems when appropriately detailed [1]. In order to achieve this ductile behavior, SMFs are typically designed to concentrate yielding in plastic hinges at the end of the beams over the entire height of the building [2], avoiding plastic hinging of the columns (which may lead to an undesirable soft story). The rest of the components of the SMF are designed (to remain elastic) with either the capacity design criteria (e.g., columns are sized based on the strong column-weak girder check) or employing the over-strength seismic load (i.e., $\Omega_o = 3$). In this way, plastification can be developed stably, without structural risk of collapse [1].

Despite the use of capacity-design principles, some column hinging is unavoidable in mobilizing a full-plastic mechanism in the SMFs [1,3]. Plastic hinges in the first story columns may be accommodated either in the lower part of the column or in the column base connection itself [3]. Typically, designers prefer the first criteria (i.e., protecting the connection) because the information related to column base connections' deformation capacity was relatively sparse. However, recent experimental programs on base connections [4–7] indicate that these connections possess significant deformation capacity (ranging from ~0.05–0.10 rad) with desirable hysteretic properties comparable with pre-qualified beam-column connections. Few studies (e.g. Refs. [3,4]) have examined the effect of the hysteretic properties of base connections on the seismic performance of SMFs, although they did not consider the influence of the gravity framing system. Falborski et al. [3] presented the results of a parametrically study that explored the influence of base connection strength, stiffness, and rotation capacity on the collapse probability of four SMFs (i.e., 4-, 8-, 12-, and 20-story). Four levels of column base connection strength were considered in this study, varying from two extreme values. The lowest level (in terms of capacity) corresponds to a base connection designed for reduced seismic loads (i.e., $R = 8$), while the strongest criteria imply a base connection seized to accommodate the plastic capacity of the attached column ($1.1R_yM_p$). Two intermediate levels of strength were considered, i.e., designing the base for $R = 3$ and $\Omega_o = 3$ (i.e., amplified seismic loads). The main finding was that similar performance (i.e., in terms of probability of collapse) for all the SMFs might be obtained by designing the base connections for over-strength seismic loads (i.e., $\Omega_o = 3$) rather than for

* Corresponding author.
E-mail address: patorresr@usfq.edu.ec (P. Torres-Rodas).

https://doi.org/10.1016/j.soildyn.2021.106654
Received 13 June 2020; Received in revised form 24 November 2020; Accepted 7 February 2021
Available online 27 February 2021

$1.1R_yM_p$ of the column (i.e., capacity design criterion), requiring that the base connections must be detailed to accommodate rotations of 0.05 rad.

Cui and Wang [8] also studied the effect of hysteretic behavior of exposed base plates on the performance of low-rise buildings, presenting the results of the NTH analysis conducted on a four-story SMF with rigid and semi-rigid bases. This archetype frame was designed based on current Japanese specifications and practices. In Japan, yielding of anchor rods is allowed when ductile anchor rods are used in the design of base connections. Results indicate that similar performance can be achieved if the SMF is designed to concentrate plasticity in either the base plate or the column's lower region.

Field evidence (e.g., the Northridge earthquake in 1994) indicates that the building's gravity system may profoundly influence their response. For instance, in the Northridge earthquake, many SMFs suffered from brittle failures at their connections. Subsequent studies (e.g. Refs. [9,10]) concluded that the buildings did not collapse (even though their connections experienced brittle failure) due to gravity framing's beneficial effect. Flores et al. [10,11] and Elkady and Lignos [12] have studied in a parametric manner the influence of gravity framing on the seismic performance of SMFs. The potential for improvement in the seismic performance of a building depends on factors such as the number of gravity columns existing, their orientation, gravity beam-column connection details, and the inter-story drift demands on each story. Among these parameters, Flores et al. [10] indicate that gravity columns (especially when they are considered continuous along with the height of the building) have the most critical influence on the seismic performance, particularly in tall buildings. Torres-Rodas et al. [13] examined the effect of column base flexibility in the presence of gravity columns on the seismic performance of an 8-story SMF. However, this study neglected the potential effect of column-base hysteretic behavior [14] as well as the contribution of PR gravity connections on the frame response [11].

In summary, studies conducted to examine the influence of the gravity framing system on the seismic performance of SMFs have mainly assumed idealized boundary conditions (i.e., fixed- or pinned-base). On the other hand, the few studies (e.g. Refs. [3,8]) that explore the effect of the hysteretic behavior of column base connections on the collapse safety of SMFs did not incorporate the influence of the gravity system in their analysis. Thus, there is a gap in knowledge concerning the consequences in SMF's behavior of reducing the base-connection strength (entailing nonlinear behavior) while incorporating the gravity framing system. Against this backdrop, this paper presents a parametric study to investigate the interrelation between the column base connection strength, rotational stiffness, and deformation capacity with the seismic performance of SMFs incorporating the effect of continuous gravity columns and partially restrained (PR) beam-column gravity connections, seeking to examine the consequences of employing a strong column – weak base connection criterion on the SMFs safety. Specifically, this paper investigates 1) the relationship between the column-base connection parameter metrics (i.e., connection strength, stiffness, deformation capacity), varying the stiffness of gravity columns, and the strength of PR beam-column connections on the collapse probability of the SMFs. 2) the sensitivity of the building's performance metrics such as inter-story drift ratios under different seismic hazard levels (i.e., Maximum Considered Earthquake, Design, and Frequently hazard levels of shaking [1,15]) to the hysteretic behavior of column-base connections, incorporating the effect of the gravity framing system.

This research differentiates with previous studies in the degree of sophistication of the models used and in the parameters investigated. First, the hysteretic behavior of column base connections is captured by using the validated models developed by Torres-Rodas et al. [16,17] for exposed base plates and Torres-Rodas et al. [18] for embedded base connections. Second, the gravity framing is explicitly considered, where the behavior of gravity PR connections is taking into account by the model developed by Elkady and Lignos [12]. While previous studies evaluate either the effect of gravity framing system or the influence of column base behavior on the seismic performance of SMFs, an investigation that assesses the impact of different column base and PR connections strength, including gravity columns (varying their stiffnesses) in the performance of SMFs, and their potential implications in design, has not been conducted to date.

Consequently, it is time to carry out this study to explore the consequences of the use of column-base as part of the energy dissipative mechanisms of buildings by weakening their strength, providing new insights into SMFs behavior. The paper begins with this introductory section, describing the past research conducted on the topic. This discussion is followed by detailing the methodology employed herein (i.e., FEMAp695 [19]), including a complete description of the models used for the archetype frames. The next section discusses the results coming from NTH analyses as well as Nonlinear Static Pushover Analyses (NSP) conducted on this investigation and their possible implications in structural modeling and design. Finally, the paper concludes by summarizing the main findings, limitations of the current research, and recommendations to overcome these limitations in future work.

2. Methodology

The primary scientific basis of this research consists of a series of NTH analyses conducted on five archetype frames varying in height (i.e., 2-, 4-, 8-, 12-, 20-story), supplemented by NSP analyses, as is presented in Fig. 1. Seeking appropriate parameter sets for archetype frame simulations is challenging due to the high number of parameters that might be varied. Thus, in this paper, the building height is considered as the only parameter selected to investigate variations among the different buildings as it appears to be the most influential factor based on previous research (e.g. Refs. [3,14]). This height ranges from 8.50 m (for the 2-story) to 79.85 m (for the 20-story). Details of the archetype frames analyzed herein are discussed next, and in the subsequent sections, the methodology for the collapse assessment is presented.

Fig. 2 illustrates the characteristics (i.e., plan view, elevation, and member size) of the archetype frames used in this investigation adopted from Ref. [20]. Even though the member size (beam and columns) changes with height, there are several characteristics in common. As per Fig. 2a, all the SMFs consist of three-bay frames located at the perimeter of the building plan. The bay width is 6.10 m, the height of the first story is 4.50 m, while the height of the rest of the stories is 3.90 m. The SMFs were designed as per ASCE 7 [21]. Thus, a dead load of 4.78 kN/m^2 was applied on all the floors, while an unreduced live load of 2.38 kN/m^2 was assigned on all floors except on the roof, where a live load of 0.95 kN/m^2 was applied. Apart from those loads, a perimeter load of 1.20 kN/m^2 was applied to simulate the cladding. The seismic design of the SMFs was carried out assuming a Response Coefficient Factor $R = Cd = 8$ and site class "D" conditions under the seismic design category D_{max} [19], which is consistent with the far-field site conditions in Los Angeles Basin area. The SMFs are controlled by inter-story drift-ratios requirements instead of strength checks. All beam-column connections were detailed as Reduced Beam Section (RBS) connections based on AISC 341 [22] and AISC 358 [23] recommendations. For more details regarding the archetype frames, refer to Ref. [20]. It is important to point out that the SMFs were designed assuming idealized base conditions, i.e., pinned-base for the 2-story building and fixed-base for the rest of the buildings. In the context of this research, this observation is essential in the interpretation of the results since the NTH analyses are conducted with different levels of column base connection strength and flexibility.

The beams and columns members are modeled as linear-elastic elements with the plasticity concentrated at their ends. Each beam-member consists of three linear-elastic elements with two nonlinear rotational springs placed at the RBS locations. These nonlinear rotational springs are aimed to capture the hysteretic behavior of the beam-column connections and are represented by the well-known Ibarra-Medina-

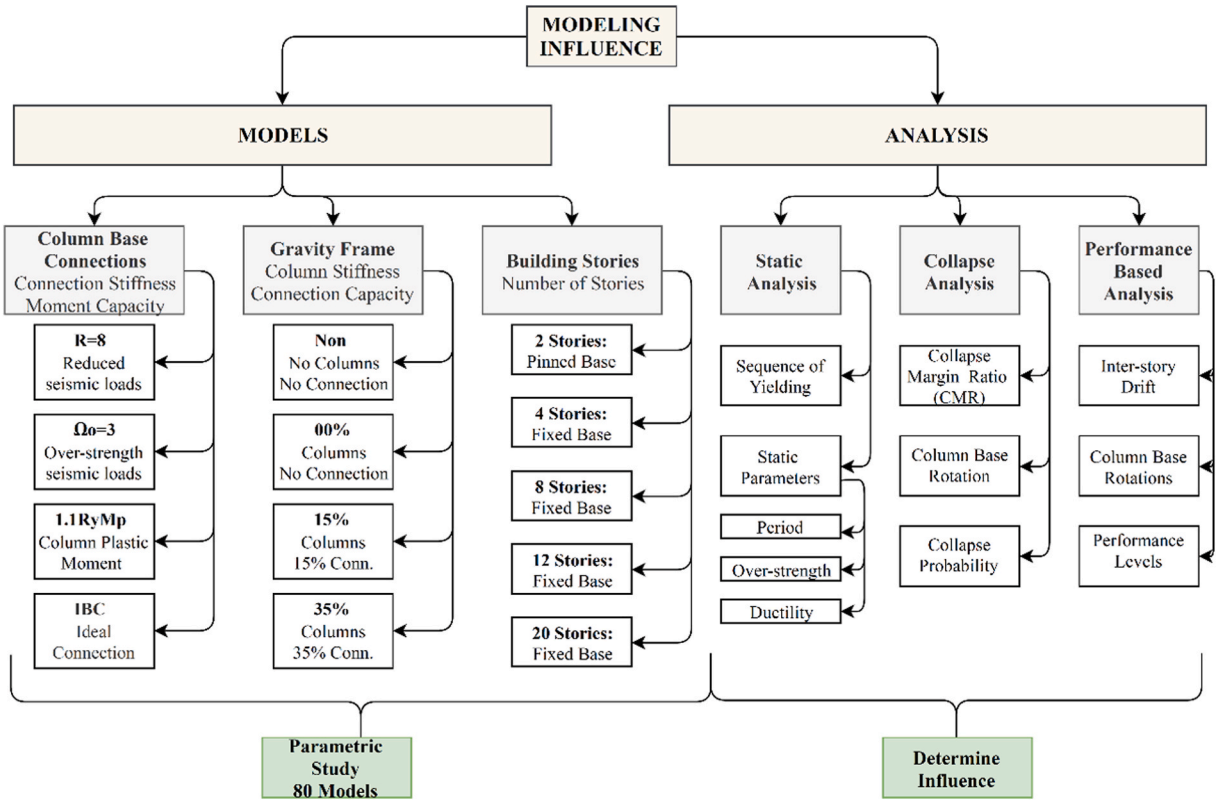

Fig. 1. Summary of the methodology of assessment.Description of the archetype frames and numerical models.

Krawinkler (IMK) bilinear model [24]. This model consists of a tri-linear backbone curve with kinematic strain hardening supplemented by rules to capture cyclic strength and stiffness deterioration. These deterioration rules were initially proposed by Ibarra et al. [24], and modified by Lignos and Krawinkler [25]. Well-developed methodologies provided in ATC [20] and illustrated in Fig. 3a1 are used to determine these springs' properties (backbone and cyclic parameters), including phenomena such as the local slenderness of the cross-section elements. The columns are modeled as linear-elastic elements with two rotational springs at their ends. These springs are similar to the springs located at the beams. However, these plastic hinges are calibrated to reflect the presence of axial load in the columns. As all uniaxial concentrated plasticity models, these models cannot capture moment-axial load interaction. Because of it, this phenomenon is represented conveniently in an approximate manner. First, the gravity loads (i.e., 1.05 P_D+0.5 P_L) are considered as an average value of the axial loads presented in the NTH analysis [26]. Next, a reduced bending strength is calculated with the interaction equations for combined forces from AISC [22]:

$$\text{If.} \quad \frac{P_g}{P_{ye}} \leq 0.20 \quad M_y = 1.15\, Z\, R_y\, F_y \left(1 - \frac{P_g}{P_{ye}}\right)$$

$$\text{If.} \quad \frac{P_g}{P_{ye}} > 0.20 \quad M_y = 1.15\, Z\, R_y\, F_y \left(\frac{9}{8}\left[1 - \frac{P_g}{P_{ye}}\right]\right)$$

Where $P_g$is the axial compressive force due to gravity loads (i.e., 1.05 P_D+0.5 P_L), and P_{ye} is the expected yield strength of the column (i.e., $R_y\, F_y\, A_g$). Thus, this reduced bending strength is used in the rotational springs at the end of the columns. In the absence of hysteretic models capable of capturing the P-M interaction response, this procedure seems to be appropriate because SMFs are drift-controlled rather than force-controlled entailing that columns are lightly loaded. Studies such as [27] show experimental data with shake tables on these systems, presents good agreement with models calibrated with the preceding procedure. The typical hysteretic behavior of a column is presented in Fig. 3a2. Panel zones are modeled as a hinged parallelogram assembly by rigid elements (to simulate the panel zone kinematics) with a nonlinear spring at one of the corners to represent shear distortions in the panel zone (This is the so-called "Krawinkler model" [25]). Beams and columns are connected to the rigid elements of the panel zone through nodes. The panel zone spring is defined by the yield, full plastic strength, and corresponding stiffness parameters (Fig. 3a3). Cyclic deterioration properties of these springs are not considered mainly because the inelastic response of panel zones is quite stable [20], which is attributed to two reasons: i) the panel zone is thick enough with respect to its other dimensions (width and depth), ii) typically, doubler plates are included in their design, avoiding local buckling. For more details about these springs, the reader is recommended to refer to Refs. [20,28]. In the frame models where the gravity framing was not incorporated, a leaning-column was used to induce P-delta effects through large displacement geometric nonlinearity. The leaning column is connected to the SMFs through rigid elements and is loaded with the gravity load (1.05 P_D+0.5 P_L) equivalent to half of the building at each floor level. Details of the mathematical models, including and neglecting the gravity framing, are presented in this paper's subsequent subsection.

Particular consideration was given to the behavior of column base connections since the information about the topic is not as extensive as other connections (e.g., beam-column connections). Consistent with current engineering practice, for low rise buildings (2-, 4- story frames) exposed base plates are the norm, while for tall buildings (8-, 12-, 20-story frames), embedded base details are preferred [3,18]. Thus, the hysteretic response of these components is simulated with the validated models developed by Torres-Rodas et al. [16] for exposed base plates and Torres-Rodas et al. [29] for embedded base connections. As shown in Fig. 3b1, these models consist of a rotational spring (connected in series with the column springs) that have a trilinear backbone curve similar to the IMK models, supplemented by rules aimed to capture the hysteretic response as well as modes of deterioration consistent with column base connections. The backbone curve of both models is defined by the base connection parameters such as moment at first yield (M_y), initial rotational stiffness (K), maximum connection moment (i.e.,

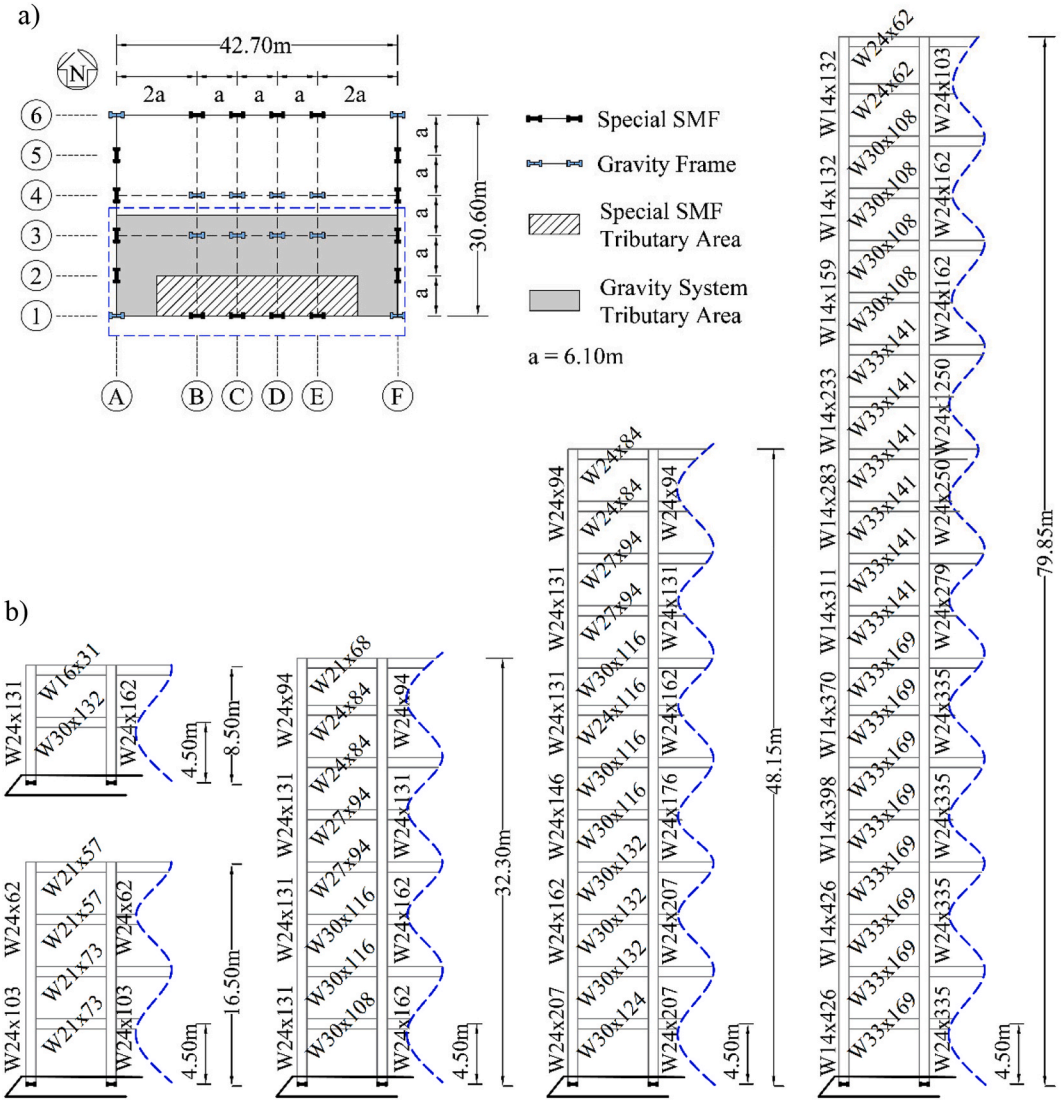

Fig. 2. Archetype frames: a) plan view, b) frame views.

M_{peak}), and rotation of the connection associated with its peak strength (θ_{peak}). Appropriate analytical methods have been proposed in the past to capture those parameters. For exposed based plates, the moment at first yield is calculated when one of their components yield, i.e., the base plate (in either the tension or compression side) or the anchor bolts. This computation is carried out iteratively. Thus, for a given axial load, the base moments are increased progressively, and the iterations stop when one of the components reaches its capacity. The maximum strength of these connections is reached when a second component yields. For more details, refer to Gomez et al. [4]. On the other hand, for embedded base connections, the moment at first yield is estimated as 70% of M_{peak} as recommended by Grilli and Kanvinde [5]. This method estimates the connection strength based on a postulated mechanism for internal force transfer, including horizontal stresses of the column flanges against the foundation, panel zone shear, and vertical bearing stresses of the embedded base plate. The initial rotational stiffness was estimated with the methodology developed by Kanvinde et al. [14] for exposed base plates and by Torres-Rodas et al. [30] for the embedded base connections. Both methods calculate the base flexibility by aggregating the deformations within the connection components. Fig. 3a4 illustrates these hysteretic models used herein. As per current design practice, the moment at first yield (instead of the maximum moment) represents the capacity of the connection [2], while passing this point (i.e., the moment at first yield) implies inelastic rotations in the connection. The comparison between the monotonic behavior of the column base connection and the column rotational spring is presented in Fig. 3c1-5 for each building.

The gravity beam and column elements are sized following a typical design (Table 1) based on ASCE 7 [31] and AISC 360 [2]. These elements are modeled as linear elastic elements with gravity column bases idealized as pinned-bases, while the gravity beam-column connections are treated as partially-restrained (PR) connections [11,12]. Previous research on the topic [12,32] indicates that the strength of these connections ranges from 15 to 35% of the plastic moment (M_p) of the gravity beam. Thus, the influence of PR connections in the seismic performance of SMFs is captured by the model developed by Elkady and Lignos [12], considering both extreme limits of the PR connection strength (i.e., 15–35% of Mp). This model consists of a trilinear rotational spring with three distinctive regions located at the ends of the gravity beams (Fig. 3b2). The first region (i.e., linear-elastic), is defined by a slip point at $0.5M_{max}$ and 0.4% rotation, while the full connection capacity (i.e., M_{max}) is reached at 3% rotation. After this point, the model plateaus up to a rotation of 8%, which is considered as an appropriate rotation limit for PR connections. No residual strength is allowed. (Fig. 3a5).

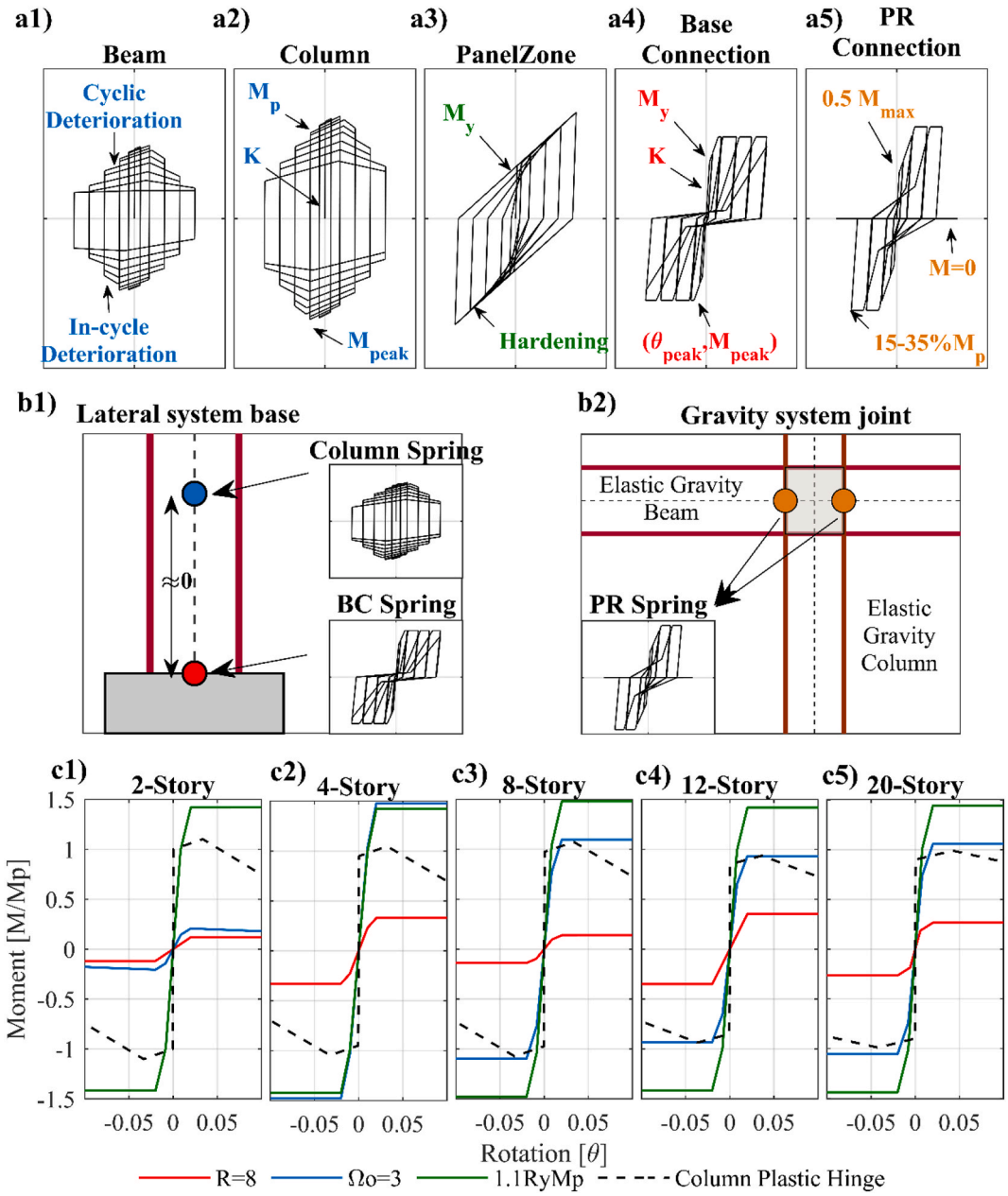

Fig. 3. Hysteretic models: a) for the beam-column connections, panel zone, column-base connections, and PR connections; b) Features of the frame simulation models; c) Normalized column-base connection strengths for each SMF.

2.1. Parameter sets investigated

All simulations can be divided into two groups 1) a set of simulations excluding the gravity system, and 2) a set of simulations including the influence of the gravity framing. In both groups, for each SMF (five in total), three different levels of column base connection strength are considered (similar criteria was used in Falborski et al. [3]). In contrast, in the second group of simulations, three cases were included for assessing the influence of the gravity system with the hysteretic behavior of base connections. Moreover, the results for the frame simulations assuming idealized boundary conditions (fixed or pinned base) were included for comparison purposes. Thus, the column base strength levels are 1) a connection designed as per current practice to accommodate the plastic capacity of the attached column, i.e., $1.1R_yM_p$; 2) a connection designed for over-strength seismic loads, i.e., $\Omega_o = 3$; and 3) a connection designed for reduced seismic loads, i.e., $R = 8$. It is anticipated based on previous work ([16,30]) that the first level of strength will not allow the development of inelastic rotations, while the last one will imply large inelastic rotations for which the connections must be detailed appropriately. Table 2 presents the results of all the base connection designs. In order to examine the influence of the gravity framing, two parameters are selected for the assessment, i.e., continuous gravity columns and PR gravity connections with different strengths. Early research on the topic (e.g. Refs. [12,32]) indicates that this strength might be in the range of 15–35%M_p. Thus, in this study, both extreme values are examined. Therefore, a total of $4 \times 4 \times 5 = 80$ simulations were conducted in this study. The details of all the simulations are summarized in Table 3. In this table, the rows indicate the cases for gravity framing assessment, while the columns, the base connection strength cases analyzed herein. The notation for the simulation is shown in each cell of the matrix. Thus, R = 8-Non is a frame simulation with base connections designed for reduced seismic loads (i.e., R = 8) and no gravity framing included. At the same time, IBC-35% represents a frame simulated with idealized boundary conditions (either fixed or pinned

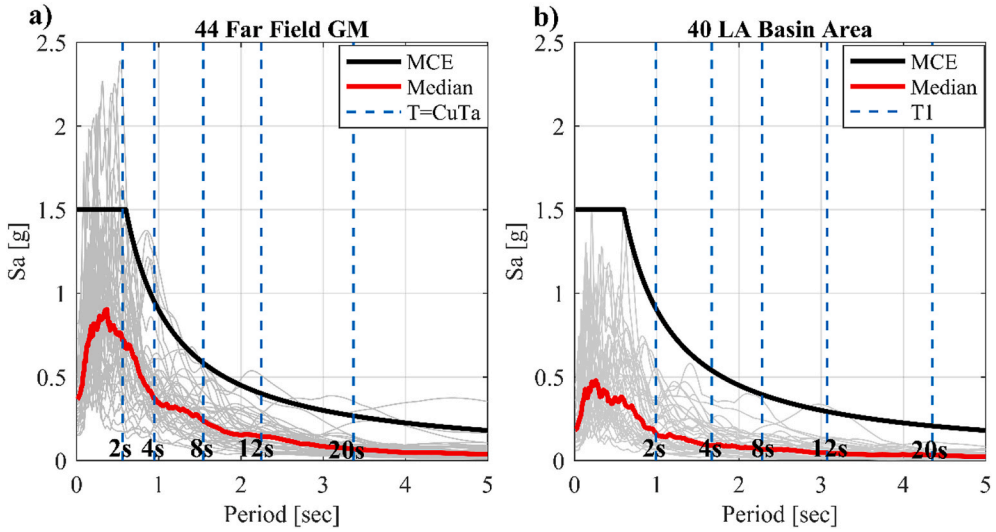

Fig. 4. Response Spectra of unscaled GMs: a) 44 Far-Field GMs from FEMAp695, b) 40 GMs from Ref. [27].

base) and with gravity framing having PR gravity connections of 35% M_p.

2.2. Nonlinear analysis of archetype frames

Two types of analyses are carried out in this paper: 1) Nonlinear Time History analysis, and 2) Nonlinear Static Pushover analysis. The NTH is mandated as per FEMAp695 methodology to assess the seismic and collapse performance of the archetype frames and is conducted herein to investigate the effects of column base strength, rotational stiffness, and ductility accompanied by the gravity columns and PR connections strength on 1) the probability of collapse of SMFs at MCE level, and 2) the seismic performance at different seismic hazard level (i.e., 2, 10, and 50% probability of exceedance in 50 years). Five archetype frames (i.e., 2-, 4-, 8-, 12-,20- story) varying in height were analyzed. First, each frame is simulated with idealized boundary conditions (i.e., pinned or fixed base) without considering the influence of the gravity framing as per current design practice. Next, each frame is analyzed considering three different levels of base connection strength (i.e., $R = 8$, $\Omega_o = 3$, and $1.1R_yM_p$) and three cases of gravity framing (i.e., gravity columns only, PR connections of 15%M_p, and 35% M_p). This parametric study results in a total of 80 mathematical models. The software OpenSees is used for all the runs since it has been extensively verified for NTH simulations [33].

A collapse assessment relative to each of the 80 simulated models was conducted following the FEMAp695 methodology. As per this methodology, incremental dynamic analysis (IDA) [34] is required. This technique consists of selecting a suite of ground motions and scale them incrementally until the structural model collapses. A suite of 44 different far-field ground motions is selected [19]. Fig. 4a illustrates the response spectra of the selected ground motions. Response metrics (e.g., inter-story drift ratios) may be generated from the IDA technique and plotted against an appropriate intensity measure (e.g., spectral acceleration at the fundamental period) to obtain the well-known IDA curves. Sidesways collapse is defined by FEMAp695 when the IDA curves become flat (or typically with a slope less than 20%) or when the inter-story drift ratios reach a value of 10% from which the structure is extremely unlikely (if not impossible) to recover [35].

In the context of this research, it is necessary to define a second limit state (apart from the sidesway collapse) in order to evaluate the effect of the deformation capacity of base connections on the frame behavior. Specifically, it is set a threshold value for their deformation capacity. As per different studies on the topic [3–5,7], an appropriate value for peak base rotations is 5%. Thus, in addition to sidesway collapse, it is presented the probability of failure defined by the exceedance of this threshold for base rotations, i.e., 5% limit. Therefore, it is assumed that the system will fail if either the drift or the base rotation limit is exceeded. This second limit state may be interpreted as a conservative assumption due to the sparse information related to the post-failure response of base connections. Studies such as Falborski et al. [3] have reported similar approaches for examining the influence of base deformation capacities on the performance of SMFs. In this manner, the median collapse capacity of each of the 80 simulations may be obtained once 22 out of 44 ground motions exceeds any of the two defined limit states. This median collapse capacity is compared with the site-hazard (i.e., probability of exceedance of 2% in 50 years) to compute the collapse margin ratio (CMR). This CMR is adjusted with the spectral shape factor (which considers the spectral shape of rare earthquakes in California) to obtain the adjusted collapse margin ratio (ACMR). Finally, the Probability of Collapse (sidesway) or failure (when the base rotations control) can be computed from the ACMR. This metric of performance is used to evaluate the safety of the archetype frames (80 combinations in total) and to understand their sensitivity to variations in column base connections strength with the inclusion of the gravity framing system (varying PR gravity connections strength).

In addition to IDA simulations, this study presents the results of the NTH analyses conducted on the archetype frames to investigate the effect of column base hysteretic behavior accompanied by gravity framing in performance metrics such as inter-story drift ratios at different seismic hazard levels of shaking (i.e., 50/50; 10/50; and 2/50). For this purpose, the suite of ground motions from the FEMAp695 methodology is considered too severe [14]. A suite of 40 ground motions selected by Medina and Krawinkler [27] is scaled up to the different seismic hazard levels mentioned before, assuming a soil type D, which is representative of the Los Angeles Basin area (Fig. 4b).

Apart from the NTH analysis, a Nonlinear Static Pushover (NSP) analysis is conducted on the models to supplement the information obtained from the NTH analysis. The NSP analysis generates "pushover curves," which provide general insights on frame response (e.g., collapse mechanism) and structural properties. As described in FEMAp695, two structural properties may be obtained from NSP analysis; 1) system overstrength (Ω_o), 2) period-based ductility (μ_t). The methodology of assessment of the archetype frames is summarized and illustrated in Fig. 5 for better comprehension. As per Fig. 5, each model is subjected to a set of ground motions. From these simulations, IM-EDP and fragility curves are generated for the performance assessment, while the NSP supplements the dynamic analysis. Each color line (or color bar) in the inner insets represents the results from a specific mathematical model.

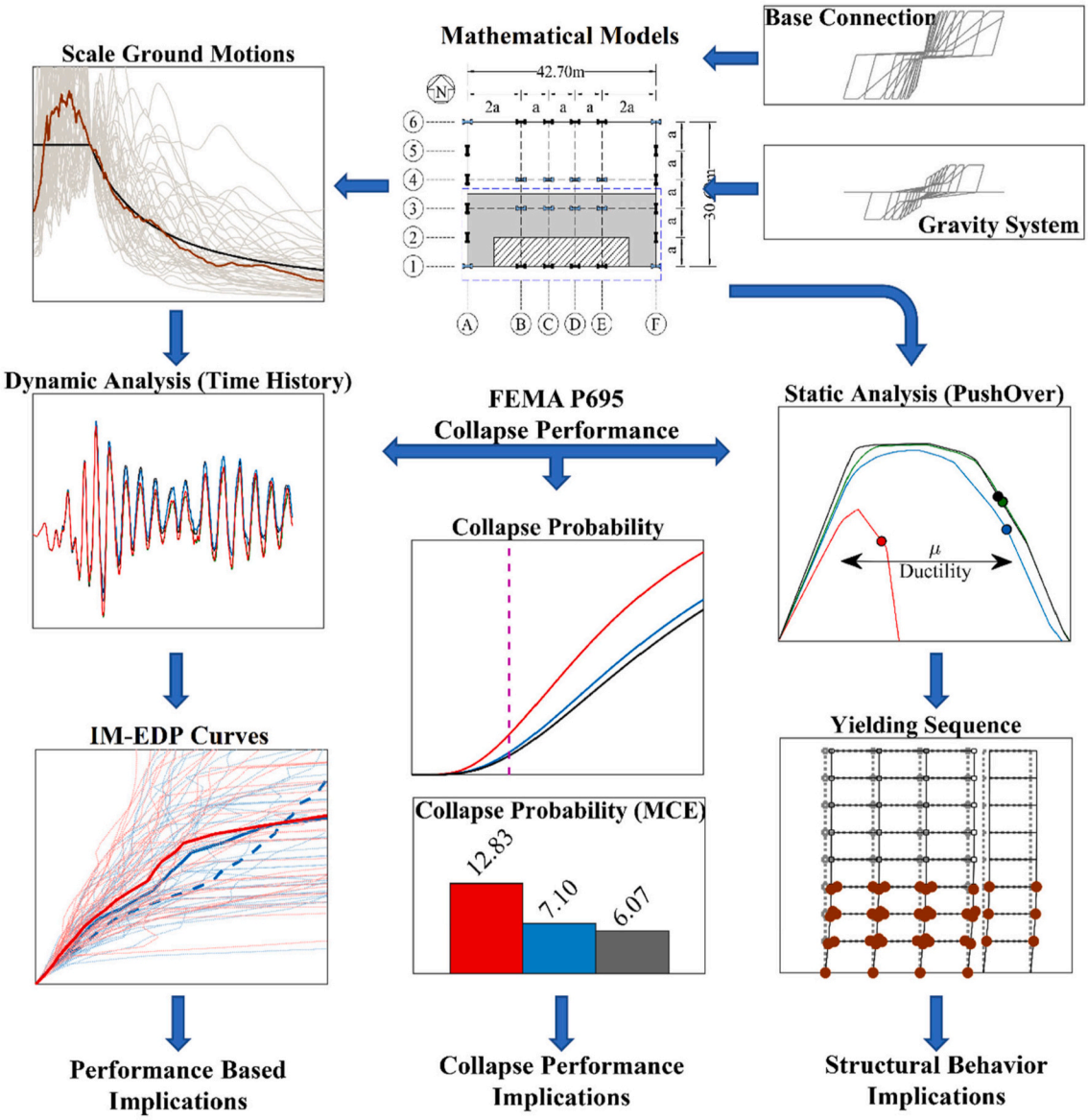

Fig. 5. Methodology flow-chart.

3. Discussion of results

This section summarizes the results obtained from the NTH and NSP analysis simulations described in the previous section with possible implications in design. Findings that represent general trends observed in all the archetypes frames are discussed first. Then, the particular observations of each archetype are outlined. This format of the discussion applies to the results obtained from both NSP and NTH analysis.

3.1. Nonlinear Static Pushover Analysis

Fig. 6, Fig. 7, and Fig. 8 detail the results from NSP analysis. Fig. 6a illustrates the pushover curves of each building (i.e., 2-, 4-, 8-, 12-, 20-story) analyzed in this paper, without the gravity system (showed with continuous lines), and with gravity columns (dash-lines in each inset) accompanied with PR connections (e.g., 35%M_p), for all the base connections strength levels (i.e., R = 8, Ω_o = 3, and 1.1R_yM_p). Fig. 6b presents further scrutiny of the pushover curve of the 8-story frame for the R = 8-Non and the R = 8–35% models, highlighting the instants that the pushover curve changes due to a yielding event. Fig. 6c traces the collapse mechanism evolution of the 8-story models indicated before (i.e., R = 8-Non and the R = 8–35%). As illustrated in Fig. 6c, the inclusion of the gravity system delays structural collapse by reducing the deformations concentrated in the first story. When the gravity system is not included (Fig. 6b1), the first yield in the SMF occurs at the RBS connections of the second floor (marker 1). As deformation is progressing, the second yield takes place in exterior column base connections (marker 2). The maximum strength in the pushover curve is reached when the rotations at the RBS connections overpass the peak strength reaching the softening branch of the hysteretic curve (marker 3), while the building reaches the zone considered to lose its capacity (below 80% of the peak strength) when the top region of the first story columns start to yield (marker 4). Because of it, a soft story is formed, which leads to structural collapse.

On the other hand, when the gravity framing is included (Fig. 6c2), structural collapse is delayed because the beams from the third and fourth floors are participating as part of the yielding mechanisms. The reason behind this improved yielding mechanism is the continuous stiffness provided by the gravity columns. In this case, the building tends to deform in the first mode shape, which entails an increase in the slope of the softening branch of the pushover curve (i.e., secondary stiffness), as is illustrated in Fig. 6b2. The collapse mechanism of this model starts

Table 1
Gravity system sections.

Columns				Columns			
Story	B3, E3	C3, D3	A1, F1	Story	B3, E3	C3, D3	A1, F1
2-Story				20-Story			
1	W14 × 43	W14 × 90	W14 × 61	**1**	W24 × 94	W27 × 336	W27 × 307
2	W14 × 43	W14 × 90	W14 × 61	**2**	W24 × 94	W27 × 336	W27 × 307
4-Story				**3**	W24 × 94	W27 × 336	W27 × 307
1	W14 × 43	W14 × 109	W14 × 68	**4**	W24 × 84	W27 × 281	W27 × 258
2	W14 × 43	W14 × 109	W14 × 68	**5**	W24 × 84	W27 × 281	W27 × 258
3	W14 × 30	W14 × 90	W14 × 53	**6**	W24 × 84	W27 × 281	W27 × 258
4	W14 × 30	W14 × 90	W14 × 53	**7**	W24 × 76	W27 × 235	W27 × 217
8-Story				**8**	W24 × 76	W27 × 235	W27 × 217
1	W18 × 76	W18 × 192	W18 × 97	**9**	W24 × 76	W27 × 235	W27 × 217
2	W18 × 76	W18 × 192	W18 × 97	**10**	W24 × 68	W27 × 194	W27 × 178
3	W18 × 76	W18 × 192	W18 × 97	**11**	W24 × 68	W27 × 194	W27 × 178
4	W18 × 76	W18 × 192	W18 × 97	**12**	W24 × 68	W27 × 194	W27 × 178
5	W18 × 50	W18 × 130	W18 × 76	**13**	W24 × 62	W27 × 161	W27 × 146
6	W18 × 50	W18 × 130	W18 × 76	**14**	W24 × 62	W27 × 161	W27 × 146
7	W18 × 40	W18 × 97	W18 × 76	**15**	W24 × 62	W27 × 161	W27 × 146
8	W18 × 40	W18 × 97	W18 × 76	**16**	W24 × 55	W27 × 129	W27 × 114
12-Story				**17**	W24 × 55	W27 × 129	W27 × 114
1	W24 × 103	W24 × 250	W24 × 176	**18**	W24 × 55	W27 × 129	W27 × 114
2	W24 × 103	W24 × 250	W24 × 176	**19**	W24 × 55	W27 × 94	W27 × 94
3	W24 × 103	W24 × 250	W24 × 176	**20**	W24 × 55	W27 × 94	W27 × 94
4	W24 × 84	W24 × 207	W24 × 146				
5	W24 × 84	W24 × 207	W24 × 146				
6	W24 × 84	W24 × 207	W24 × 146				
7	W24 × 68	W24 × 131	W24 × 117				
8	W24 × 68	W24 × 131	W24 × 117				
9	W24 × 68	W24 × 131	W24 × 117				
10	W24 × 55	W24 × 94	W24 × 94	**Beams (2-, 4-, 8-, 12-, 20-story)**			
11	W24 × 55	W24 × 94	W24 × 94	**Story**	**A-B, E-F**	**B–C, C-D, D-E**	
12	W24 × 55	W24 × 94	W24 × 94	**All**	W24 × 94	W 16 × 36	

Table 2
Base connection strength.

Stories	Strength Level	Moment Strength Ext (kN.m)	Int (kN.m)
2	R = 8	261.45	296.02
	$\Omega_o = 3$	454.31	493.74
	$1.1R_yM_p$	2612.09	3276.38
4	R = 8	382.96	435.65
	$\Omega_o = 3$	1736.65	1958.08
	$1.1R_yM_p$	1927.24	1963.62
8	R = 8	309.04	292.35
	$\Omega_o = 3$	1167.36	2309.99
	$1.1R_yM_p$	2612.09	3276.38
12	R = 8	966.46	1074.48
	$\Omega_o = 3$	2526.68	2847.79
	$1.1R_yM_p$	4145.49	4200.06
20	R = 8	607.22	1295.37
	$\Omega_o = 3$	3277.92	5158.65
	$1.1R_yM_p$	6006.31	7106.91

Table 3
Model Matrix: Parameter sets investigated.

MODEL MATRIX		BASE CONNECTION			
		R = 8	$\Omega_o = 3$	$1.1R_yM_p$	IBC[a]
GRAVITY SYSTEM	L.F.[b]	R = 8-Non	$\Omega_o = 3$-Non	$1.1R_yM_p$-Non	IBC-Non
	L.F.+G.C.[d]	R = 8-00%	$\Omega_o = 3$-00%	$1.1R_yM_p$-00%	IBC-00%
	L.F.+G.C.+P.C. 15%[c]	R = 8–15%	Ω_o = 3–15%	$1.1R_yM_p$-15%	IBC-15%
	L.F.+G.C.+P.C. 35%	R = 8–35%	Ω_o = 3–35%	$1.1R_yM_p$-35%	IBC-35%

[a] I.B.C. = Idealized Boundary Condition (Fixed or Pinned).
[b] L.F. = Lateral Frame.
[c] P.C. = Partial Connection of the gravity system.
[d] G.C. = Gravity Columns.

with the first yield of the RBS connections on the second floor (marker 5), followed by the base connection yielding (marker 6). As the deformations progress, the RBS connections from the third and fourth floor starts to yield. The system reaches its peak (marker 7) when the RBS connections at the second floor get into the softening region while the PR gravity connections start to yield. After this point, as the deformations are increased, the columns at the first, second, and third stories start to yield (Fig. 6b2). Finally, the building loses its capacity (marker 8) when the PR beam-column gravity connections fail. It is important to point out that gravity columns remain essentially elastic up to the system's collapse. This latter observation is consistent with the findings reported by Flores et al. [11]. A closer inspection of Fig. 6b indicates that the deformation capacity of the system due to the inclusion of the gravity framing is increased by a factor of two. Similar trends are observed in the rest of the frames (Fig. 6a). As discussed in the preceding lines, the inclusion of gravity framing, in general, modify the collapse mechanism enforcing the building to deform in the first mode of shape.

As detailed in the previous section of this paper, two limit states are considered in this study for each mathematical model 1) sidesway collapse and 2) base-connection failure. Thus, Figs. 7 and ***8*** show the sensitivity of the metrics obtained from NSP analysis (i.e., period-based ductility and system overstrength) to the different parameter sets investigated herein, considering both limit states. Each inset on these figures presents the results of one of the buildings (e.g., 2- story), while each color-bar represents one model simulation detailed in Table 3 for the sidesway collapse limit state (as defined by FEMAp695). On the other hand, the yellow markers show the period-based ductility calculated based on the base-connection failure limit state. As per Fig. 7, the period-based ductility (μ_t) appears to change once column-base and PR gravity connections strength change (for both limit states). This sensitivity may be attributed to the fact that gravity columns tend to reduce inter-story drift concentrations enforcing the building to deform in its first mode shape. At the same time, an increase in base connection strength entails an increment in its rotational stiffness, increasing its capacity of deformation. A closer examination of Fig. 7 reveals interesting findings. First, for the 2- and 8- story frames with bases designed for R = 8, and $\Omega_o = 3$ (where plastic rotations are allowed), the period

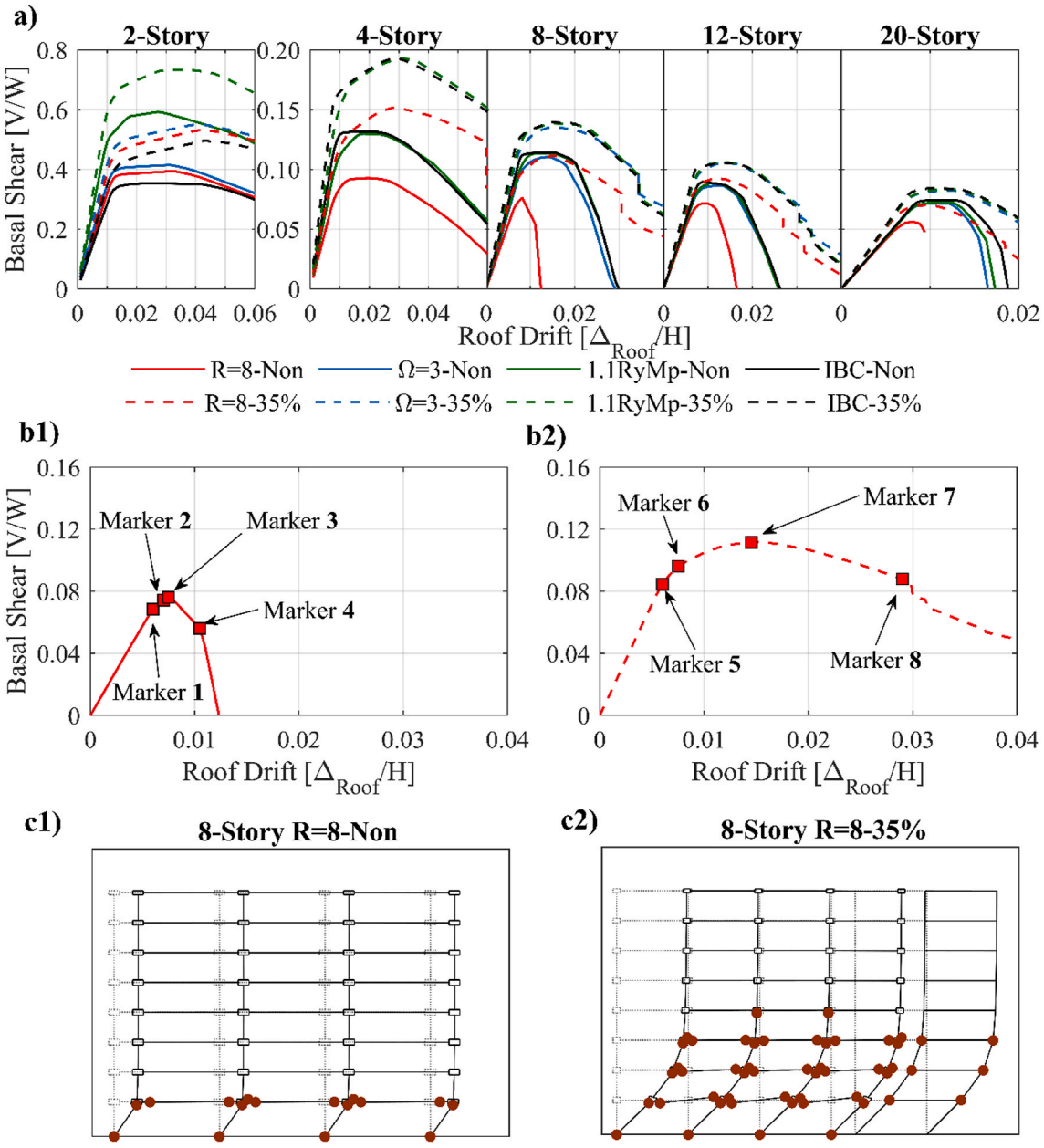

Fig. 6. NSP analysis: a) Pushover curves for each model; b) Detailed Pushover curve of the 8-Non and 8–35% models; c) Structure deformation and yielding mechanisms of the 8-Non and 8–35% models.

based-ductility determined based on the base-connection failure limit state reaches its peak when gravity columns are included, but the PR gravity connections are neglected. This phenomenon may be attributed to the fact that the hinges' rotations located at the lower region of the first story column do not reach the softening branch (i.e., secondary stiffness). Thus, the plastic rotations are higher in the base plates rather than in the column. Because of this, the inclusion of PR gravity connections in this condition increases the base plate rotations. On the other hand, in the rest of the frames (4-, 12-, and 20- story), it is observed that the hysteretic models located at the lower region of the columns reach their softening branches. Thus, column rotations are higher than base connection rotations, implying that the PR gravity connections increases the ductility of the system since base connection rotations are delayed.

From the results of NSP analyses, it can be inferred that there are four possible cases once base connection behavior is incorporated: 1) If the base connection is sized with the capacity design criteria (i.e., $1.1R_yM_p$), plastic rotations are concentrated only in the lower part of the first story columns; 2) Either the column and the base connection yield, but the column does not reach the softening branch; 3) Either the column and the base connection yield, but the column rotations overpass the peak rotation strength getting into the softening branch; 4) If the connection is designed for reduced seismic loads (i.e., R = 8) plastic rotations are concentrated on the base connection. Cases 2 and 3 take place when the base connections are designed with the overstrength seismic load (i.e., $\Omega_o = 3$).

Similar trends are observed in Fig. 8 for the system overstrength (Ω_o), which relies on the peak base shear (rather than base rotations). An increase in PR or base connection strength entails an increase in this system overstrength parameter. It is worth indicating that in several of the 80 combinations analyzed, the system overstrength is lower than three, which is the value prescribed by AISC 341 [2] for SMFs. Specifically, all the combinations for the 20-story building have overstrength values less than three. The same observation is valid in the 4- and 12-story frames when the PR gravity connections strength is neglected.

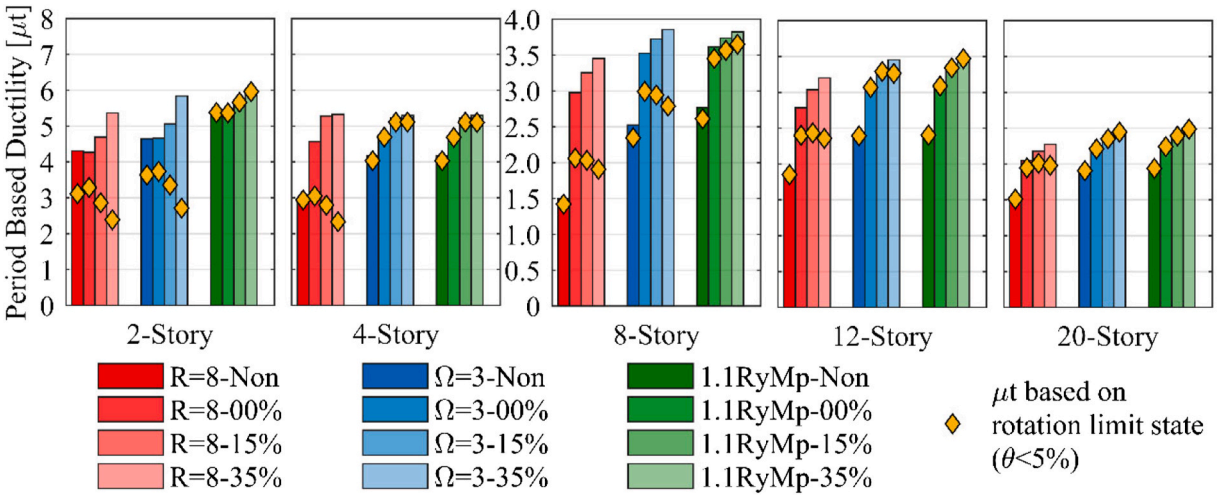

Fig. 7. Sensitivity of Period-base ductility to each parameter investigated.

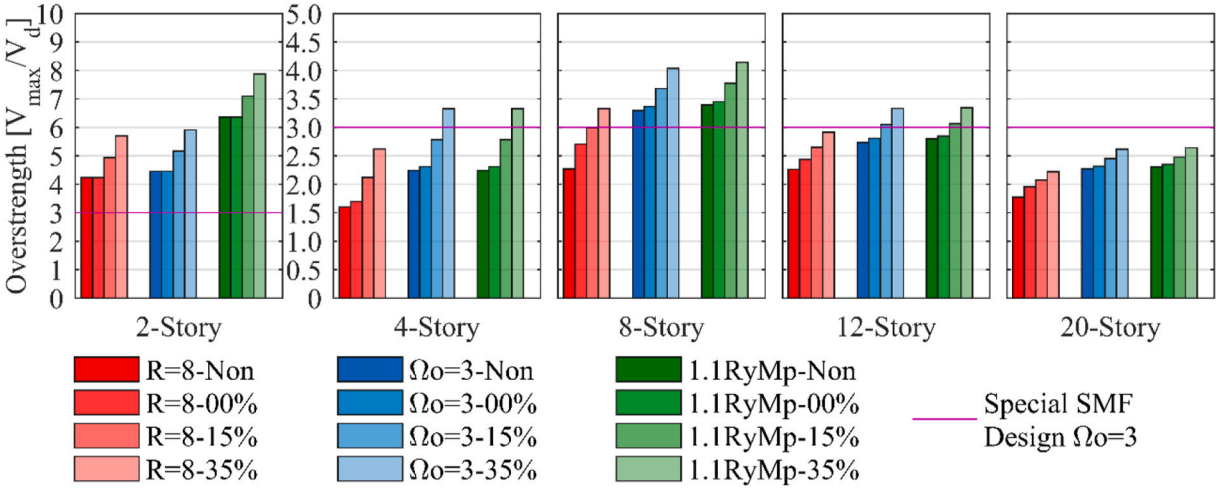

Fig. 8. Sensitivity of Overstrength to the parameters investigated.

The only frame that presents values of system overstrength higher than three for all the simulation combinations is the 2-story. This effect may be explained by how the building was designed, i.e., assuming a pinned base. Thus, in the simulations, the rotational base stiffness incorporated provides an additional source of frame strength neglected in the building design.

3.2. Nonlinear Time History Analysis

This discussion starts by commenting on the sensitivity of the first period of the buildings to the parameters investigated. Then, the results from the NTH simulations are presented. These results are divided into two parts; 1) the collapse assessment of the 80 model combinations at MCE level (i.e., 2/50 years), and 2) the seismic performance of the frame simulations at Frequent Earthquake (i.e., 50/50), Design Hazard (i.e., 10/50) and MCE level of shaking (i.e., 2/50). The findings from the collapse assessment of the archetype frames are examined before the performance evaluation under the different seismic hazard levels.

Table 4 shows the sensitivity of the building's first period to the base connection strength and the inclusion of gravity framing. In general, an increase in base connections strength entails an increase in their rotational stiffness, which leads to a decrease in the first period of the building. Also, this effect is observed when the PR gravity connections are added to system (15% and 35%M_p). On the other hand, the presence

Table 4
First period of the Archetype Frames.

		First Period of the Archetype Frames				
		2-Story	4-Story	8-Story	12-Story	20-Story
Frame Model	R = 8-Non	0.93	2.18	2.75	3.40	4.58
	R = 8-00%	0.93	2.18	2.75	3.40	4.58
	R = 8–15%	0.88	1.98	2.56	3.20	4.33
	R = 8–35%	0.86	1.90	2.48	3.10	4.19
	Ω = 3-Non	0.86	1.86	2.46	3.21	4.45
	Ω = 3-00%	0.86	1.86	2.46	3.21	4.45
	Ω = 3–15%	0.82	1.70	2.32	3.04	4.22
	Ω = 3–35%	0.80	1.62	2.25	2.94	4.08
	$1.1R_yM_p$-Non	0.69	1.86	2.42	3.18	4.44
	$1.1R_yM_p$-00%	0.69	1.86	2.42	3.18	4.44
	$1.1R_yM_p$-15%	0.66	1.70	2.28	3.01	4.20
	$1.1R_yM_p$-35%	0.64	1.62	2.21	2.91	4.07
	IBC-Non	0.99	1.67	2.28	3.07	4.35
	IBC-00%	0.99	1.67	2.28	3.07	4.35
	IBC-15%	0.93	1.52	2.15	2.90	4.12
	IBC-35%	0.91	1.45	2.08	2.80	3.98

of gravity columns only tends to linearize the deformed shape of the building, improving its performance but has a negligible effect on this dynamic property.

Fig. 9 shows a summary of the results from the collapse assessment; thereby the sensitivity of the parameters investigated is illustrated. The collapse margin ratio (CMR) is presented first because this value depends only on the model behavior (Fig. 9a). Then, the collapse probability is calculated using the uncertainty values for Special SMF (Fig. 9b). As per the FEMAp695 methodology, the acceptance criteria correspond to a probability of failure of less than 10%. As a general observation, the inclusion of continuous gravity columns positively affects the performance of all the models analyzed herein. At the same time, an increase in either column base or PR gravity connections strength tends to decrease the probability of collapse of the archetype frames. In the context of this research, it is essential to state that although a decrease in base-connection strength entails an increase in base flexibility, this effect may be counteracted by the high deformation capacity that these connections pose. Particular observations of all model simulations are detailed next.

When the gravity framing is not included in the analysis, the following observations are pertinent:

- For the frames analyzed with idealized boundary conditions, i.e., pinned or fixed-base, the collapse probabilities of most of the frames are on the verge of the acceptance criteria (i.e., ~10%) except for the 20-story building, which shows a probability of collapse equal to 16%. These values are virtually the same as the ones reported by NIST [20]. Thus, these results serve as a way to validate the models developed herein to study the effect of column base hysteretic behavior with the gravity framing system incorporated in the simulations.
- When the values of column-base connection strength decrease, the probability of collapse tends to increase because an increment in base flexibility tends to drop down the inflection point in the moment diagram of the first story columns, this phenomenon produces an increment in the moments at the top region of the first story columns and potentially leads to a soft story mechanism. Specifically, for the frames analyzed with base connection strength of R = 8, collapse probabilities of all models are in unacceptable levels (>25%) with the exception of the 2-story frame, as illustrated in Fig. 9b. These results are similar to the ones reported by Falborski et al. [3] in of their study (i.e., Prob of failure: 35% for the 4-story; 90% 8-story; 65% 12-story; and 80% 20-story). As per Falborski et al. [3], an increment in base connection deformation capacity (from 0.01 to 0.05 rad) entails a decrease in the system collapse probability. Thus, the problem associated with an increment of column-base flexibility may be counteracted by levering their high deformation capacity (set as 5% in this study) and incorporating these connections as part of the dissipative energy mechanisms.
- Frames simulated with base strength levels corresponding to $\Omega_o = 3$ and $1.1R_yM_p$ lead to a relatively similar performance in terms of collapse probability. These results are illustrated in Fig. 9b, and it may be attributed to the fact that the rotational stiffnesses for both strength levels are not significantly different, providing enough rigidity to the bases to enforce the inflection point of the moment diagram of the first story columns to remain relatively close to the middle column height. Besides, at the collapse verge, the rotations monitored at the base connections are less than 5%. This finding implies that base-connections designed for $\Omega_o = 3$ must be detailed to hold rotations of 5% if the gravity framing is not included in the analysis. These results agree with the values reported by Falborski et al. [3].

Interesting results are observed in the frame simulations when the gravity framing system is included. The following observations are relevant in the context of this research:

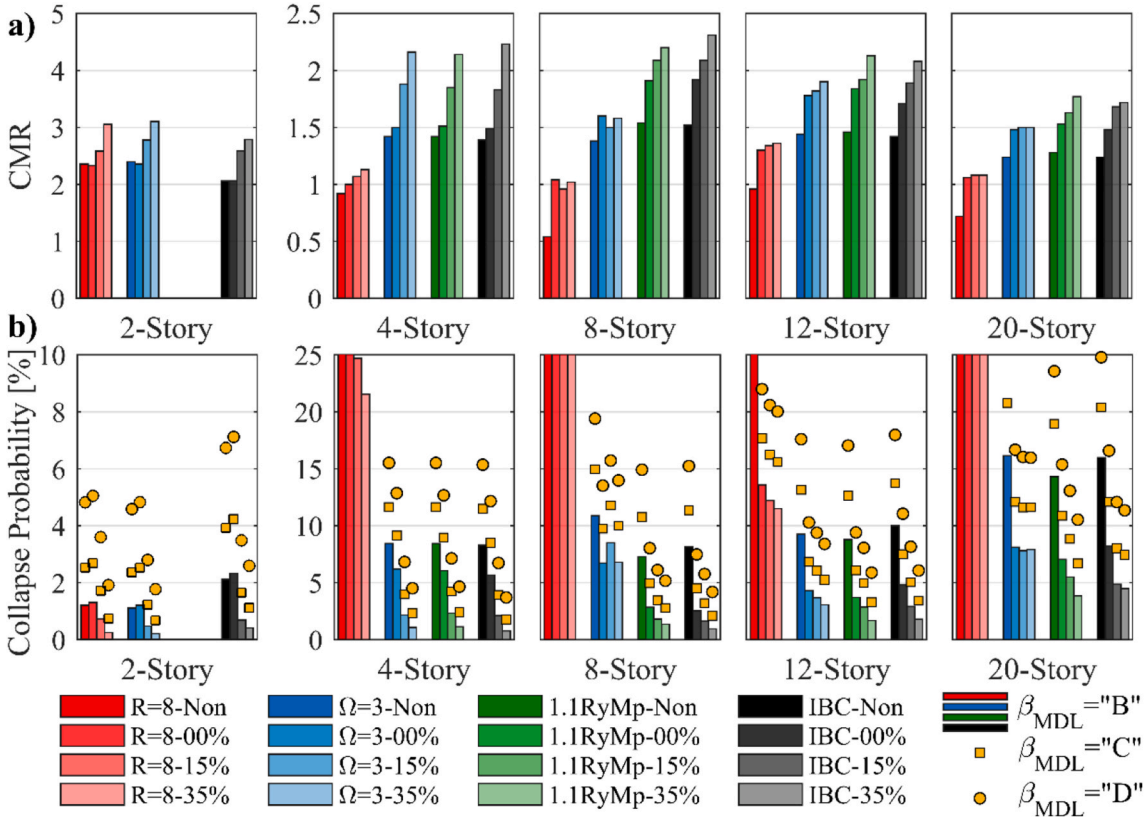

Fig. 9. Collapse Assessment summary: a) Collapse Margin Ratio, b) Probability of Collapse for each model simulation.

- The performance of all the parametric combinations is significantly improved (i.e., probability of collapse decreases) due to the beneficial influence of gravity columns with PR beam-column connections. This phenomenon may be attributed to the fact that continuous stiffness of gravity columns tends to lead the SMFs to deform in the first shape mode preventing (or delaying) soft story mechanisms. Apart from that, PR connections contributed to an increase in the system overstrength and the deformation capacity of the building, improving its resilience. Thus, the beneficial contribution of the gravity framing in the analysis permits a reduction in the column base connections strength (from $1.1R_yM_p$ to $\Omega_o = 3$) in a safe manner, leveraging their ductility as part of the dissipative energy system.
- Fig. 9b indicates that the sole inclusion of the gravity columns (i.e., neglecting the contribution of PR connections) reduces the collapse probability of all the model simulations significantly. This inclusion is able to alter unacceptable values (even as high as 92%) to values relatively close to the border of acceptance criteria (i.e., ~15%). For instance, when the 20-story building is analyzed with a base connection strength of R = 8, without gravity columns, it presents a probability of collapse of 90%. However, when the same model is analyzed with the inclusion of the gravity columns, the probability of collapse drops down to 26%. This general trend is observed for the rest of the frames. In general, the influence of gravity columns is more profound in tall buildings (12-, 20-story) rather than in the low-rise ones.
- The beneficial effect of PR gravity connections can also be inferred from Fig. 9. For all frames (with the exception of 8-story), an increment in the PR gravity connections strength entails a reduction in their probability of collapse. Interestingly, when PR connections are considered (for both cases of analysis), the 4-, and 12-story buildings present collapse probabilities as low as 3% or even less than that value. A closer inspection of Fig. 9a indicates that the effect of PR gravity connections strength is more pronounced in the low-rise buildings rather than in tall buildings. Specifically, in the tall buildings, the difference in the results when including gravity connections compared with the case that only considers gravity columns is in the order of 1%.
- In all frames, the base strength level of R = 8 leads to unacceptable results, with the only exception of the 12-story building. As per Fig. 9, the collapse probability in all the models is greater than 20%, except for the 12-story building. In this frame, when PR gravity connections are considered, the probability of collapse is ~12% (close to acceptance criteria). A closer examination of these analyses cases (i.e., R = 8) reveals that the base rotations limit state controls (by far) the system failure. If the base rotations are neglected in the analysis (i.e., sidesway collapse controls), the probabilities of collapse are at acceptable levels. Specifically, if PR gravity connections are considered, the probability of collapse in all frames is less than 8%. However, base rotations in all models at this level of deterioration are close to 10%. This observation would imply that a significant reduction of base demands (i.e., from $1.1R_yM_p$ to R = 8) would be possible only if base connections can hold rotations as high as 10%. Experimental results by Gomez et al. [4] and Trautner et al. [7] indicate that this value for rotation capacity is not unrealistic. However, to date, there are no guidelines (such as for pre-qualified connections) that guarantee those levels of ductility in column base connections. Thus, in the author's opinion, the threshold of 5% for base rotations assumed in this paper is appropriate as a limit state.

As per FEMAp695 [19], the computation of the collapse probability includes many sources of uncertainty. Specifically, the sources are the Record-to-Record Variability, Designs Requirements, Test Data, and Modeling Uncertainty. The combination of all of them gives the Total Uncertainty. Thus the collapse probability values presented before were computed using a total uncertainty where the model uncertainty (β_{MDL}) was the type "B" recommended by NIST [20] for Special SMF. This value is used due to the extended laboratory test that supports the pre-qualified beam-column connection hysteretic behavior. In the case of column-base connections and the gravity system, the experimental data available is limited. Because of it, the authors validated the collapse probability of the mathematical models using more severe model uncertainties (i.e., β_{MDL} = "C" and β_{MDL} = "D") to examine their possible consequences in the results. These results are presented for each simulation model in Fig. 9b with a square and circle marker, respectively. Fig. 9b shows that acceptable values of collapse probability are achieved only in the models, which include PR gravity connection (15% M_p), and when the base connection does not yield (i.e., $1.1R_yM_p$).

A notorious trend is observed when the base connections are designed with the overstrength seismic load (i.e., Ω_o = 3). For this strength level, the influence of the gravity system in the overall system's behavior is limited by the base connection rotation limit state because, as mentioned before, the gravity columns tends to linearize the deformed shape of the building, which increases the base rotation demands (except for the 4-story). This might be explained because the plastic rotations at the lower part of the first story columns do not overpass the softening branch (i.e., secondary stiffness in the IMK hysteretic model). Consequently, plastic rotations in the base connection are higher than that in the column, and the connection failure limit state is reached before the sidesway collapse. This observation was inferred from the insights obtained from the NSP analysis. In contrast, for the 4-story frame, the first story columns reach the softening zone before the base connections overpass their rotation capacity. Thus, an additional set of runs was conducted on these models (i.e., $\Omega_o = 3$) to determine the influence of different degrees of gravity column stiffnesses, modifying the inertias of the designed gravity columns of the 8-, 12-, and 20-story buildings by a factor (α). This value increases the gravity column's rigidity until the system presents no further improvement based on a static Pushover analysis (i.e., α = Saturation). In Fig. 10a the influence of a robust gravity system on the static behavior shows an increment mainly on the ductility of the system, which leads to an increment of the deformation capacity before reaching the 5% base rotation limit state (diamond marker in Fig. 10a).

The collapse performance of these models shows a consistent improvement despite the limit state-controlled (i.e., either sidesway collapse or base connection failure) when the inertia of the gravity columns increases. Fig. 10b and c show the collapse margin ratio and the collapse probability, respectively, where an increment in gravity columns stiffness entails an improvement in the system performance. Specifically, if this stiffness is incremented twice, the probability of collapse is reduced by more than half. For instance, the probability of collapse of the 12-story building reduces from 16% (for α = 1) to 5.5% for α = 2. These collapse probabilities were calculated with a model uncertainty (β_{MDL}) type "B" corresponding to special SMF. However, due to the sensibility of the collapse probability to the uncertainty, different β_{MDL} (type "C" represented with squares and type "D" with circles) were used to verify the influence of gravity column stiffness in the buildings. For the case of α = 2, the probabilities of collapse are between ~8 and 12% in the three SMFs interrogated. However, the improvement with a gravity system until the saturation point (i.e., α = Saturation) yields into acceptable collapse probabilities even in the worst modeling uncertainty case (i.e., β_{MDL} = " D″) as it is noticeable in Fig. 10c.

3.3. Performance assessment at different seismic hazard levels

Fig. 11 shows the results of the performance assessment for all model combinations (80 in total) at different seismic hazard levels. Specifically, the influence of the parameter sets (gravity system and column base connection behavior) on the inter-story drift ratios were examined at 1) Frequent Earthquake level (i.e., 50/50); 2) design-level (i.e., 10/50 hazard); and 3) at MCE level of shaking (i.e., 2/50). This second set of runs complement the quantitative information presented before in the

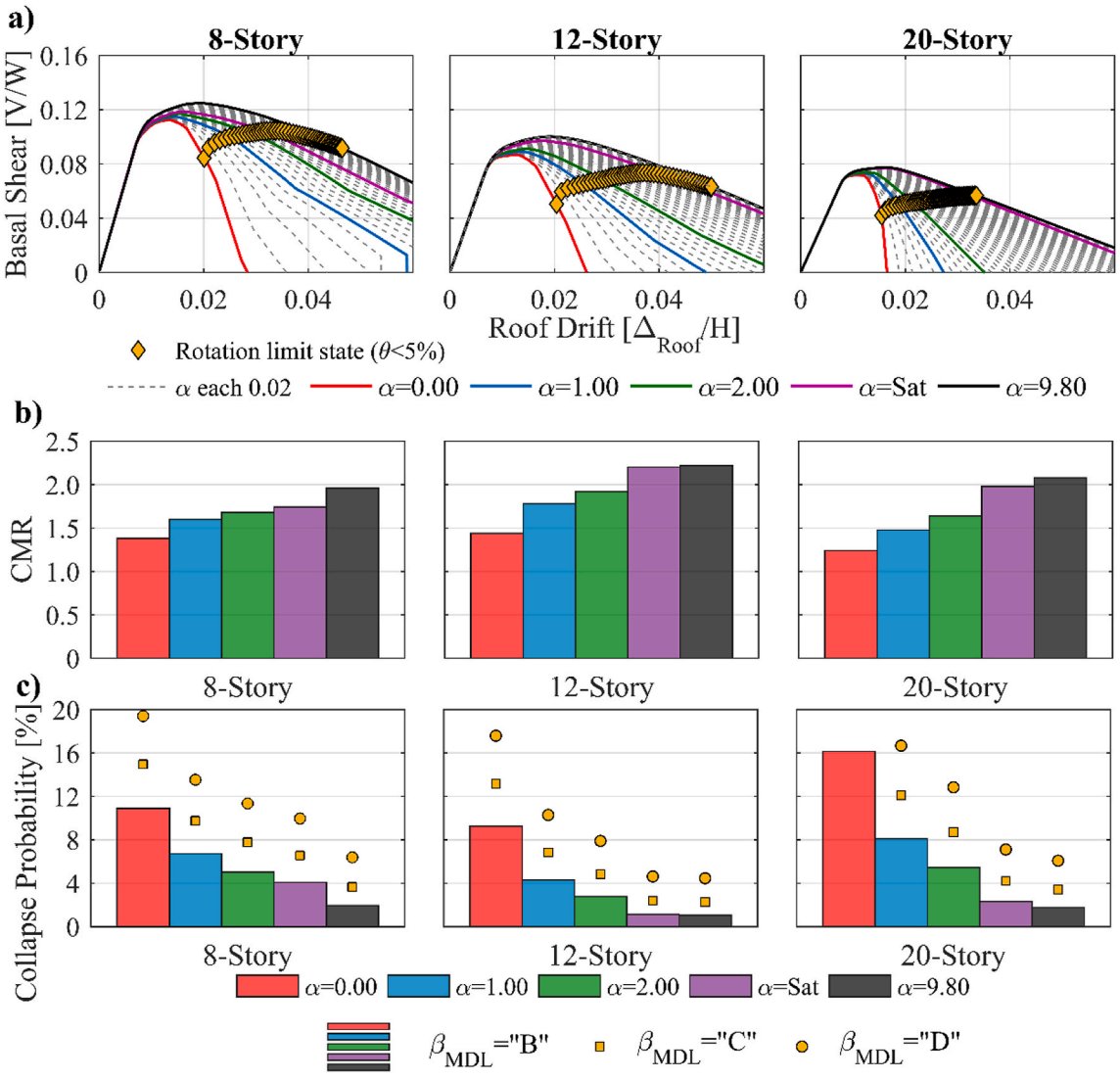

Fig. 10. Influence of α factor on a) NSP, b) CMR, c) Collapse Probability.

IDA simulations conducted as per FEMAp695 methodology. Fig. 11a presents the median values of the maximum inter-story drift ratios of each building, while Fig. 11b and c show the median of the maximum base connection rotations and the number of collapses/failures at MCE level, respectively. Each inset of Fig. 11 provides the results of a specific frame (i.e., 2-, 4-, 8-, 12-, 20- story), while the bars (varying in color depending on the model analyzed) represents the results at the Design-level, and the markers (circle or square) the result for the Frequent and MCE levels of shaking, respectively. As per Fig. 11a, it seems that, in general, an increment in base connection strength decreases the median peak inter-story drift ratios due to an increase in column base stiffness. This result confirms the findings reported by Zareian and Kanvinde [14] that the base flexibility influences Engineering Demand Parameters (EDP), such as inter-story drift ratios. However, a comparison between the inter-story drift ratios obtained from the analysis for the models with base connections designed for $\Omega_o = 3$ and $1.1R_yM_p$ reveals that their median peak values are relatively close. Moreover, these values are close to the ones corresponding to the results from fixed-base models. A closer inspection of Fig. 11a indicates that the effect of the gravity framing system on the inter-story drift ratios is relatively modest, except for the models with bases designed for R = 8. It appears that under relatively low levels of deformation, the beneficial effect of the gravity system is minor. This phenomenon may be explained (referring to Fig. 6) because the gravity framing increases the slope of the softening branch (i.e., secondary stiffness) in the "pushover curve." Thus, this benefit on the system behavior may be observed only at higher levels of deformations.

Results of the 2-story building indicate that for all parametric combinations, median peak inter-story drift ratios are below the prescribed code limits (i.e., <2.5%) at the Design level of Shaking. This was expected because the building was designed considering a pinned base. For this 2-story frame, each level of column base connection strength provides a rotational stiffness that was neglected in the design. On the other hand, the rest of the buildings presents in most of the cases median peak inter-story drift ratios above the allowable value (i.e., 2.5%), even if the gravity framing is included. Specifically, for base connections designed for R = 8, all models exceed the allowable code drift limit. For the cases of $\Omega_o = 3$ and $1.1R_yM_p$, when the models include the PR connections, the median values of the inter-story drifts are close to the code limit. However, without the inclusion of PR gravity connections, this metric exceeds the maximum code limitation. Although these observations are important in the context of this research, their implications are beyond the scope of this paper because it is related to the building design rather than the parameter set investigated herein. Consequently, this topic deserves further examination in future research.

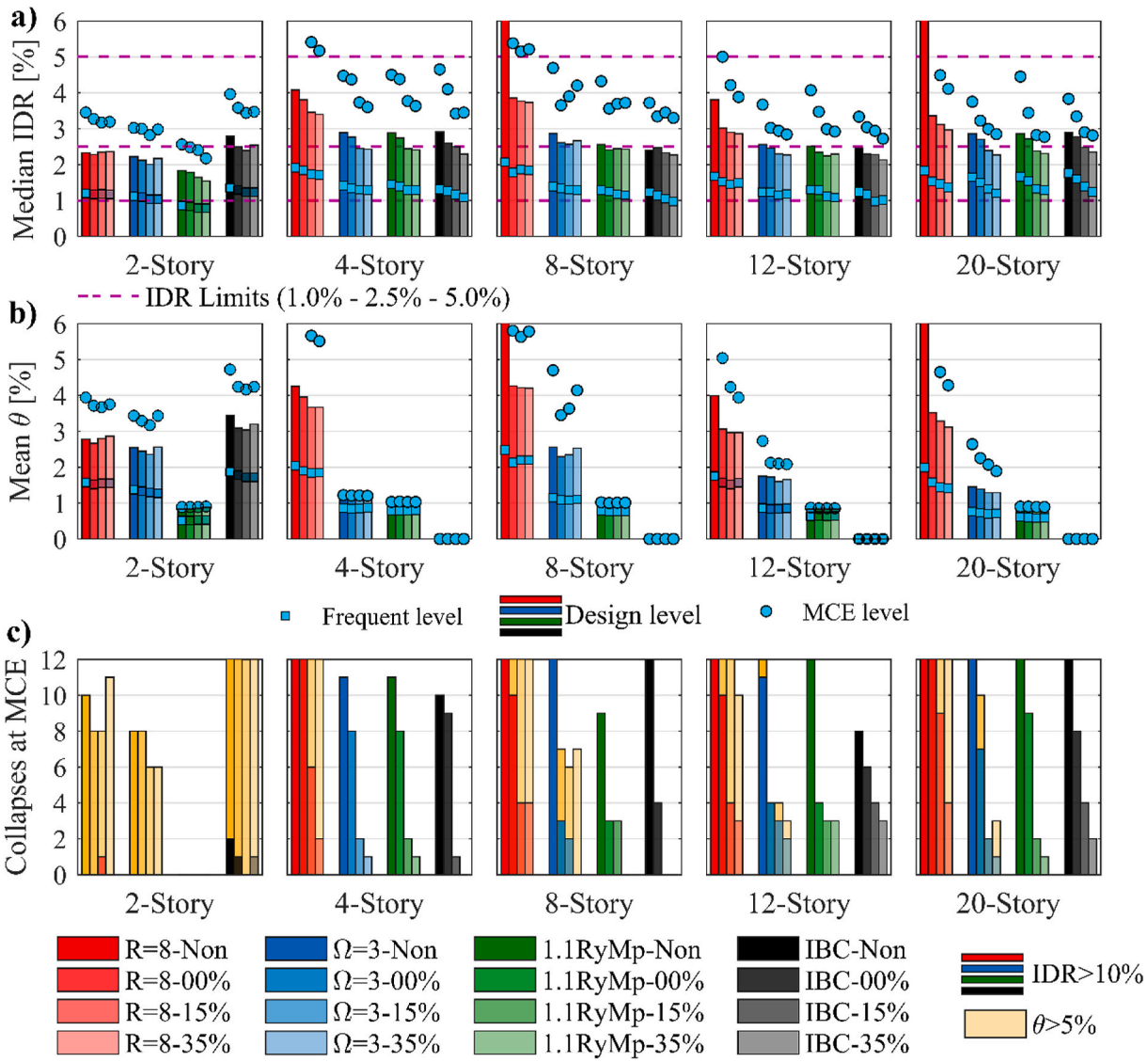

Fig. 11. Results from Performance Assessment of each model a) Median IDR, b) Median Column Base Rotations (θ), c) Number of Collapse at MCE level.

4. Summary and conclusions

This paper presents a parametric study conducted on five archetype frames varying in height (i.e., 2-, 4-, 8-, 12-, and 20- stories). The study examines, for each mentioned frame, the interrelations between column base connection strength, stiffness, deformation capacity, gravity columns stiffness, and PR beam-column gravity connections strength on 1) the probability of collapse of SMFs following the FEMAp695 methodology, and 2) inter-story drift ratios at different seismic hazard levels of shaking (i.e., Frequent, Design and Maximum Considered Earthquake). The archetype frames share some common characteristics such as plan view, story height, and loading, as indicated earlier in the paper, while the building height is the sole varied parameter between all the frames.

First, all the frames were analyzed, excluding the gravity system and considering idealized boundary conditions, i.e., pinned or fixed base. Second, three different levels of column base strength were considered, i.e., R = 8, Ω_o = 3, and $1.1R_yM_p$. The latter case corresponds to the current design criteria, which aim to protect the connection itself, promoting yielding at the lower region of the first story column. The other two cases (i.e., R = 8, Ω_o = 3) entails inelastic rotations at the column base connections. Then, all frames were analyzed for each base connection strength level, including the gravity columns and PR gravity connections. Two different levels of PR gravity connection strengths were examined, i.e., 15% and 35% of M_p of the gravity beam, while three levels of gravity stiffnesses supplemented the analysis. These parametric combinations lead to a total of 80 frame simulations, including four levels of column base strength and two levels of PR gravity connections strength.

In general, it is observed that an increase in base flexibility tends to alter force/moment distribution, and consequently, the collapse mechanism. Deformations are concentrated in the first story, which may lead to soft stories. However, this phenomenon is counteracted when the gravity columns and PR beam-column connections are included in the analysis. The NTH results indicate that the gravity system profoundly affects (positively) the SMFs behavior, especially at large deformations, by reducing the probability of collapse. Thus, the gravity framing system permits to leverage the column-base connection ductility safely as part of the energy dissipative mechanisms.

Among the three base strength levels considered in this study (i.e., R = 8; Ω_o = 3; $1.1R_yM_p$) it appears that the case Ω_o = 3 is the most promising. For this strength level, the probabilities of collapse vary between ~6 and 9% for the models with gravity connections of 15%M_p and between ~3 and 7% for the models with gravity connections of 35% M_p. Consequently, from the author's analysis, the demands for the

design of column base connections can be reduced from the capacity design criteria (i.e., $1.1R_yM_p$) to the overstrength seismic load (i.e., $\Omega_o = 3$) safely when the gravity framing system is incorporated in the analyses (assuming that column bases can hold 5% rotations). Designing column base connections for $\Omega_o = 3$ instead of $1.1R_yM_p$ would entail a strength reduction of up to 50% (Refer to Table 2). These findings suggest that perhaps the current design practice of sizing column base connections with the capacity design criteria (i.e., $1.1R_yM_p$) to remain elastic is unjustified, given their desirable hysteretic properties. Thus, the column base connections may be incorporated as part of the fuses in SMFs. In fact, this "strong column-weak connection criteria" has already been used in seismic regions such as Chile, where field evidence indicates that base connections detailed based on this design criterion have performed appropriately in major earthquakes [36]. Although experimental programs have shown that these connections pose high deformation capacity (between 4 and 8%), research on ductile base connections details deserves further scrutiny. Besides, considering the profound influence of gravity framing system on metrics such as the probability of collapse, perhaps it may be worthed to select this system not only for carrying gravity loads, instead it may be sized to target performance objectives. This last observation can be particularly important in the retrofit of existing buildings.

The findings outlined in this paper are subjected to several limitations that must be considered in order to generalize its results. The paper considers a limited number of archetype frames (which share their plan view), being their height the sole parameter changed among all the buildings. It may limit the generality of these findings considering that other design solutions are possible for the same conditions. Other factors that may limit the generalization of the results are 1) bias due to ground motion effects (including the effects of vertical acceleration component of ground motions), and 2) modeling assumptions such as the use of concentrated plasticity (vs. distributed plasticity) models, and 3) this research does not address the effect of soil-structure interaction.

Declaration of competing interest

The authors declare that they have no known competing financial interests or personal relationships that could have appeared to influence the work reported in this paper.

Acknowledgements

The authors are thankful for the financial support received from Universidad San Francisco de Quito through the 2020 'Poligrant' program.

References

[1] Bruneau M, Uang C-M, Sabelli R. Ductile design of steel structures. New York; Toronto: McGraw-Hill; 2011. http://www.myilibrary.com?id=335745. [Accessed 1 October 2018].
[2] AISC. Specification for structural steel buildings. 2016.
[3] Falborski T, Torres-Rodas P, Zareian F, Kanvinde A. Effect of base-connection strength and ductility on the seismic performance of steel moment frames. 2020.
[4] Gomez I, Deierlein G, Kanvinde A. Exposed column base connections subjected to axial compression and flexure. 2010. https://datacenterhub.org/resources/1239.
[5] Grilli D, Kanvinde A. Tensile strength OF embedded anchor groups: tests and strength models. Charles Pankow Foundation; 2015.
[6] Kanvinde AM, Grilli DA, Zareian F. Rotational stiffness of exposed column base connections: experiments and analytical models. J Struct Eng 2012;138:549–60. https://doi.org/10.1061/(ASCE)ST.1943-541X.0000495.
[7] Trautner CA, Hutchinson T, Grosser PR, Silva JF. Investigation of steel column–baseplate connection details incorporating ductile anchors. J Struct Eng 2017;143:04017074. https://doi.org/10.1061/(ASCE)ST.1943-541X.0001759.
[8] Cui Y, Wang F, Yamada S. Effect of column base behavior on seismic performance of multi-story steel moment resisting frames. Int J Struct Stabil Dynam 2019;19:1940007. https://doi.org/10.1142/S0219455419400078.
[9] Leon RT. Composite connections. Prog Struct Eng Mater 1998;1:159–69. https://doi.org/10.1002/pse.2260010208.
[10] Flores F, Charney F, Lopez-Garcia D. The influence of gravity column continuity on the seismic performance of special steel moment frame structures. J Constr Steel Res 2016;118:217–30. https://doi.org/10.1016/j.jcsr.2015.11.010.
[11] Flores FX, Charney FA, Lopez-Garcia D. Influence of the gravity framing system on the collapse performance of special steel moment frames. J Constr Steel Res 2014;101:351–62. https://doi.org/10.1016/j.jcsr.2014.05.020.
[12] Elkady A, Lignos DG. Effect of gravity framing on the overstrength and collapse capacity of steel frame buildings with perimeter special moment frames: effect OF gravity framing ON steel buildings with perimeter SMF. Earthq Eng Struct Dynam 2015;44:1289–307. https://doi.org/10.1002/eqe.2519.
[13] Torres-Rodas P, Flores F, Zareian F. Seismic Response of Steel Moment Frames considering gravity system and column base flexibility. Los Angeles: California; 2018.
[14] Zareian F, Kanvinde A. Effect of column-base flexibility on the seismic response and safety of steel moment-resisting frames. Earthq Spectra 2013;29:1537–59. https://doi.org/10.1193/030512EQS062M.
[15] Fema 350. Recommended Seismic Design Criteria for New Steel Moment-Frame Buildings; 2000.
[16] Rodas PT, Zareian F, Kanvinde A. Hysteretic model for exposed column–base connections. J Struct Eng 2016;142:04016137. https://doi.org/10.1061/(ASCE)ST.1943-541X.0001602.
[17] Torres-Rodas P, Fayaz J, Zareian F. Strength resistance factors for seismic design of exposed based plate connections in special steel moment resisting frames. Earthq Spectra 2020;36:537–53. https://doi.org/10.1177/8755293019891714.
[18] Torres-Rodas P, Zareian F, Kanvinde A. A hysteretic model for the rotational response of embedded column base connections. Soil Dynam Earthq Eng 2018;115:55–65. https://doi.org/10.1016/j.soildyn.2018.08.015.
[19] FEMA P-695. Quantification OF building seismic performance factors. 2009.
[20] NIST. Evaluation of the FEMA P-695 methodology for quantification of building seismic performance factors. Gaithersburg, MD: National Institute of Standards and Technology; 2010.
[21] Structural engineering institute. Minimum design loads for buildings and other structures. Reston, VA: American Society of Civil Engineers/Structural Engineering Institute; 2006.
[22] AISC. Seismic provisions for structural steel buildings. 2010.
[23] AISC. Prequalified connections for special and intermediate steel moment frames for seismic applications. 2010.
[24] Ibarra LF, Medina RA, Krawinkler H. Hysteretic models that incorporate strength and stiffness deterioration. Earthq Eng Struct Dynam 2005;34:1489–511. https://doi.org/10.1002/eqe.495.
[25] Lignos DG, Krawinkler H. Deterioration modeling of steel components in support of collapse prediction of steel moment frames under earthquake loading. J Struct Eng 2011;137:1291–302. https://doi.org/10.1061/(ASCE)ST.1943-541X.0000376.
[26] NIST. Guidelines for nonlinear structural analysis and design of buildings. part IIa - steel moment frames. Gaithersburg, MD: National Institute of Standards and Technology; 2017. https://doi.org/10.6028/NIST.GCR.17-917-46v2.
[27] Medina R, Krawinkler H. Seismic demands for nondeteriorating frame structures and their dependence on ground motions. Stanford, California: The John A. Blume Earthquake Engineering Center; 2003.
[28] Gupta A, Krawinkler H. Prediction of seismic demands for SMRFs with ductile connections and elements. SAC Steel Project; 1999.
[29] Torres-Rodas P, Zareian F, Kanvinde A. Seismic demands in column base connections of steel moment frames. Earthq Spectra 2018;34:1383–403. https://doi.org/10.1193/062317EQS127M.
[30] Rodas PT, Zareian F, Kanvinde A. Rotational stiffness of deeply embedded column–base connections. J Struct Eng 2017;143:04017064. https://doi.org/10.1061/(ASCE)ST.1943-541X.0001789.
[31] ASCE 7. In: Minimum design loads and associated criteria for buildings and other structures. Reston, Virginia: American Society of Civil Engineers; 2017.
[32] Liu J, Astaneh-Asl A. Moment–rotation parameters for composite shear tab connections. J Struct Eng 2004;130:1371–80. https://doi.org/10.1061/(ASCE)0733-9445 (2004)130:9(1371).
[33] Mazzoni S, McKenna F, Scott MH, Fenves GL. OpenSees command language manual. 2006.
[34] Vamvatsikos D, Cornell CA. Applied incremental dynamic analysis. Earthq Spectra 2004;20:523–53. https://doi.org/10.1193/1.1737737.
[35] Kanvinde A. Micromechanical simulation of earthquake induced fractures in steel structures. Stanford, California: Blume Earhquake Engineering Center; 2004.
[36] Greg Soules JG, Bachman RE, Silva JF. Chile earthquake of 2010: assessment of industrial facilities around concepción. Reston, VA: American Society of Civil Engineers; 2016. https://doi.org/10.1061/9780784413647.